Theor Appl Climatol
DOI 10.1007/s00704-014-1186-z

ORIGINAL PAPER

# The effect of deforestation on the regional temperature in Northeastern China

**Lingxue Yu · Shuwen Zhang · Junmei Tang · Tingxiang Liu · Kun Bu · Fengqin Yan · Chaobin Yang · Jiuchun Yang**

Received: 19 February 2014 / Accepted: 24 May 2014


**Abstract** Land cover change, as one of the most important driving forces to climate change, has become the research focus of the global environmental change research and global land project. More researchers studied on the global influence of Land-Use and Land-Cover Change and proved that land use change occurred at different temperature zones may produce different climate effects. For example, deforestation in tropical areas would lead to higher temperatures as the decreasing of evapotranspiration caused by the reduction of roughness and the decreasing of drag coefficient and leaf area index while, in boreal areas, similar deforestation would cause lower temperature as the increasing of albedo particularly during winter with the snow cover. However, the impact of deforestation in the temperate regions on the climate still existed uncertainty and the impacts of deforestation at different humidity conditions on climate has not explored yet. From this perspective, this article used Weather Research and Forecasting model to simulate the impact of deforestation on the temperature of Northeastern China. In this study, we designed two scenarios in July and December, respectively: One was simulated without human intervention, and the second one was simulated with the current forest covers. The results showed that the temperature in both summer and winter showed a decreasing trend when the conversion of forest to farmland occurred in northeastern China. In order to further explore the humidity impacts on the temperature, we performed sample analysis on humid, sub-humid, and semi-arid regions. According to the results, the maximum variation of temperature was found in humid areas, especially in December when the temperature decreased around 4–5 °C, while the change in semi-arid and sub-humid areas is relatively small.

## 1 Introduction

Land use/cover change is an essential driving factor for climate change (Fu 2003; Feddema et al. 2005a; Dirmeyer et al. 2010; Mahmood et al. 2010) by modifying the temperature, runoff, atmospheric circulation, and exchange of energy and momentum at different scales. Many research organizations believe that the feedback between land and atmosphere system can help us better understand the basic mechanisms of climate formation (Mahmood et al. 2006; Niyogi et al. 2009). In order to understand comprehensively the interaction between land use change and climate change, more observations, measurements, and simulation are necessary and required (Zhang et al. 2008; Paeth et al. 2009).

Numerous models have been used to simulate the climate change caused by land use/cover change (Baidya Roy 2003; Cooley et al. 2005) mainly at global scales. For instance, general circulation models (GCMs), the most widely used climate model which predict feedbacks of land cover change from large-scale atmospheric circulation (Feddema et al. 2005b; Lawrence et al. 2007). The Community Climate System model is another widely used climate model which involved the land surface process that can work as a stand-

L. Yu · S. Zhang (✉) · K. Bu · F. Yan · C. Yang · J. Yang
Northeast Institute of Geography and Agroecology, Chinese Academy of Sciences, Changchun 130012, People's Republic of China
e-mail: zhangshuwen@neigae.ac.cn

L. Yu · F. Yan · C. Yang
University of Chinese Academy of Sciences, Beijing 100049, People's Republic of China

J. Tang
Department of Geography and Environment Systems, University of Maryland, Baltimore County, Baltimore, MD 21250, USA

T. Liu
Bureau of Land and Resources of Linyi City, Linyi 276000, China

Published online: 03 July 2014

alone module to test the significant impacts of land cover and land use change on climate (Collins et al. 2006). With the research demands of regional land cover change and their corresponding climate impact, more detailed information on climate change are required. Regional climate models with finer spatial resolutions (the best resolution can reach 20 km or higher) become important tools to investigate the regional climate phenomenon caused by land cover and land use change (Steiner et al. 2005; Correia et al. 2007). Weather Research and Forecasting (WRF) has been adapted for simulating regional climate in recent years. With the land surface model embedded in the model, it can show the meteorological features such as diurnal cycle of temperature (Zeng et al. 2011) and precipitation, etc., as well as express the influences of regional issues in better resolution to give better understanding of the coupling relationship between land and atmosphere (Das et al. 2011; Subin et al. 2011).

In summary, land use/cover change affect climate through two aspects: biogeochemical process and bio-geophysical process. The former one represents the changes in the surface physical characteristics (e.g., vegetation) caused by land use/cover change, which can change the albedo; surface roughness; evapotranspiration; and the exchange of radiation, water, and momentum between land and atmosphere, resulting in the climate change (Betts 2001; Bonan 2008). The latter mainly focuses on the carbon dioxide emissions caused by land use/cover change, which may increase or decrease the long-wave radiation and further alter climate conditions (Sitch et al. 2005; Bala et al. 2007). This study focused on the biogeochemical process on regional scales.

Most of the analysis and simulations make a common conclusion on the impact of land use/cover change on climate at both regional and global scales (Wang et al. 2013; Wu et al. 2013; Deng et al. 2013): On one hand, the forest degradation or deforestation would reduce the surface roughness, the drag coefficient, and surface evapotranspiration, which would result in warming climate (Hahmann and Dickinson 1997; Li and Molders 2008); on the other hand, the increasing surface albedo would reflect more radiation away from Earth and would bring the cold climate effect (Bonan 1997; Davin and de Noblet-Ducoudré 2010). In tropical latitudes, the warming effect caused by increase of surface evapotranspiration is more significant than the cold effect caused by the albedo increase, and therefore, the influence is eventually manifested as rising temperature (Comarazamy et al. 2013). In the boreal areas, surface albedo increased significantly, especially in the snow-covered areas (Barnes and Roy 2010), hence the cooling effect caused by deforestation performs dominantly and finally led to the temperature decrease (Bounoua et al. 2002; Swann et al. 2010). For the mid-latitudes, there exists uncertainty of the climate response caused by land cover changes, and the dominant climate effects may vary in different seasons (Lamptey et al. 2005; Betts et al. 2007). Most of these studies, either through numerical simulations or field observations, studied the impact of land use/cover change on the climate influence under different heat conditions or under different latitudes. Therefore, if this relationship were detected under either different wet conditions or under different longitudes, it will be interesting to make a conclusion on the relationship between climate change and land use/cover change impacts. In this article, we used WRF model to explore the impact of deforestation on the temperature in different seasons and under different aridity conditions, in order to provide support for the rational land allocation and land-use decisions on regional scale.

This article includes five parts. The first part introduced the research contents and the significance of the study; the second part proposed the study area and data preparation and processing, and the third section described the scenario-based simulation method. Next, we analyzed and compared the results of different simulation scenarios under different seasons with different aridity conditions. The last part of this article summarized the main results and conclusion.

## 2 Study area and data processing

### 2.1 Study area

The study area, Northeastern China, ranges from longitudes 115°05′E to 135°02′E and from latitudes 38°40′N to 53°34′N, including Liaoning province, Jilin province, Heilongjiang province, and eastern Mongolia (Fig. 1). The total area of the northeastern China is 1,450,000 $km^2$, with a total population of 120 million. The study area is located in the temperate and monsoon climatic zones with a typical continental climate (Ye et al. 2001; Wang et al. 2010). The average annual precipitation and temperature are about 400–700 mm and −1.1 °C–4.4 °C, respectively, with a long, extremely cold, and dry winter and short, mild, and moist summer. The zonal characteristics of precipitation and temperature enable the formation of different aridity conditions in northeastern China, which would be explained in the next section.

Historically, the northeastern China was a wide forest area with small population before the deforestation process associated with the construction of railway and timber production from the first half of the twentieth century (Dai et al. 2006; Wang et al. 2010). The population growth, as well as the expanding food demand, has caused a rapid reduction in grassland and forest during the last 50 years, potentially affecting the future regional environment and climate with a rapidly changing landscape pattern. The coexistence of forest, pasture, and agriculture lands exhibits mosaic and fragmental pattern of land use, turning the study area into a significant area to climate change.

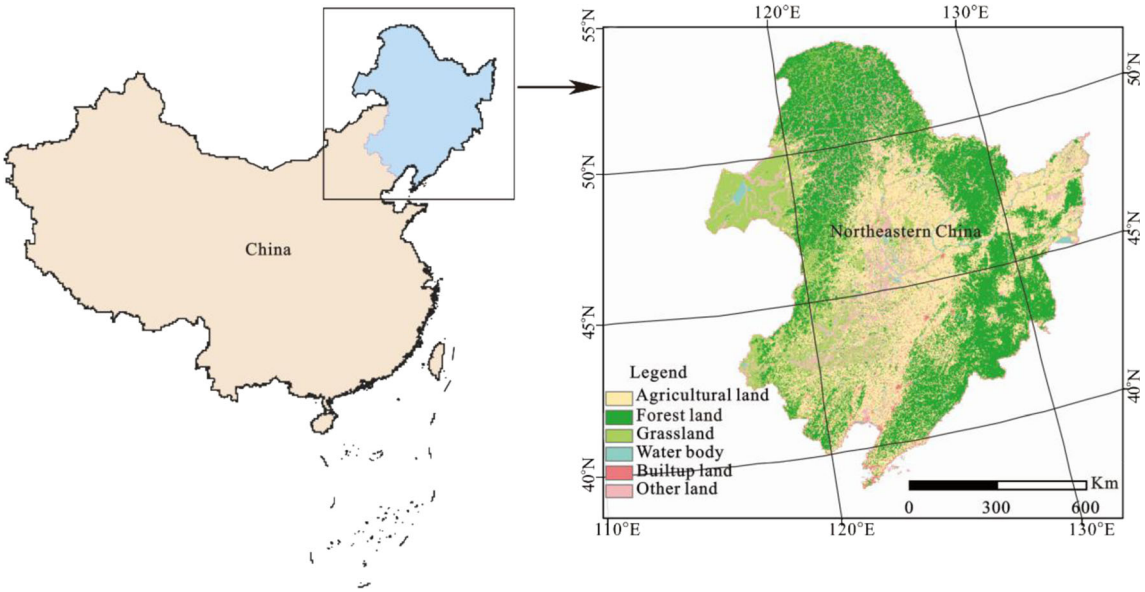


**Fig. 1** The study area, Northeastern China

## 2.2 Data preparing and processing

### *2.2.1 Aridity index*

Aridity index (AI) is an indicator characterizing the degree of wetness and dryness of a region which has been applied in geography and ecology for a long time. In recent years, it has been used as a significant climate indicator in the global change research, especially in climate change, drought, and desertification. The AI map was derived from the accumulated temperature $T$ and precipitation R when the daily average temperature is higher than 10 °C using Eq. 1.

$$\mathrm{AI} = \frac{0.16 \times \sum T_{\geq 10^{\circ}\mathrm{C}}}{\sum R_{\geq 10^{\circ}\mathrm{C}}} \quad (1)$$

Where $\sum T_{\geq 10^{\circ}\mathrm{C}}$ and $\sum R_{\geq 10^{\circ}\mathrm{C}}$ indicate active accumulated temperature and precipitation when daily average temperature is steadily higher than 10 °C. The AI represents the ratio between the potential evapotranspiration and precipitation. The accumulated temperature and precipitation were collected from weather stations and interpolated into grid format by using three-dimensional quadric surface modeling coupled with residual interpolation at a significance level of $\alpha$=0.001 (Yu et al. 2004). Generally, AI of humid climate zone is often lower than 1.00, while 1.00–1.50, 1.50–3.50, and higher than 3.50 correspond to the semi-humid climate, semi-arid climate, and arid climate zones, respectively. We reclassified the climatic aridity zone of the study area using the grid computing and reclassification tools of ArcGIS (Fig. 2).

According to Fig. 2, the study area includes three climate types: humid, semi-humid, and semi-arid climate zones. In the following sections, we will analyze the impact of deforestation on regional temperature in these three different aridity zones.

### *2.2.2 Surface parameter data*

With different surface parameters, the land cover types can influence the climate change through the biological geophysical processes. Taking into account the regional nature of the Northeastern China and accuracy of the simulation, it is necessary to make improvements to the surface parameters that are closely related to land cover types such as LAI and Albedo.

As the MODIS land cover data (2003), the original data in WRF, cannot represent the real situation of land cover, we replaced the original data with the land cover data in 2010 produced in our previous study with the overall classification accuracy from 80 % to 88 % (Fig. 3). Then we calculated the LANDUSEF (the percentage share of each land cover type in a grid), LANDINDEX (the dominate land cover type in each grid), and LANDMASK (water body mask data) at different spatial resolutions based the land cover dataset above using the batch processing of ArcGIS. Finally, we replaced the land cover data through MATLAB.

The surface albedo, the key factor in surface radiation balance and energy balance, was derived from MODIS products including MCD43B3, MOD04, and MOD03. The real albedo can be calculated as the interpolation between the black sky albedo and white sky albedo (Eq. 2):

$$\alpha = \alpha_{\mathrm{w}} \times S(z, b, od, amt) + \alpha_{\mathrm{b}} \times (1 - S(z, b, od, amt)) \quad (2)$$

Here, $\alpha$ represents the surface real albedo; $\alpha_{\mathrm{w}}$ is white sky albedo; $\alpha_{\mathrm{b}}$ is the black sky albedo; $S$ is the fraction of diffusion

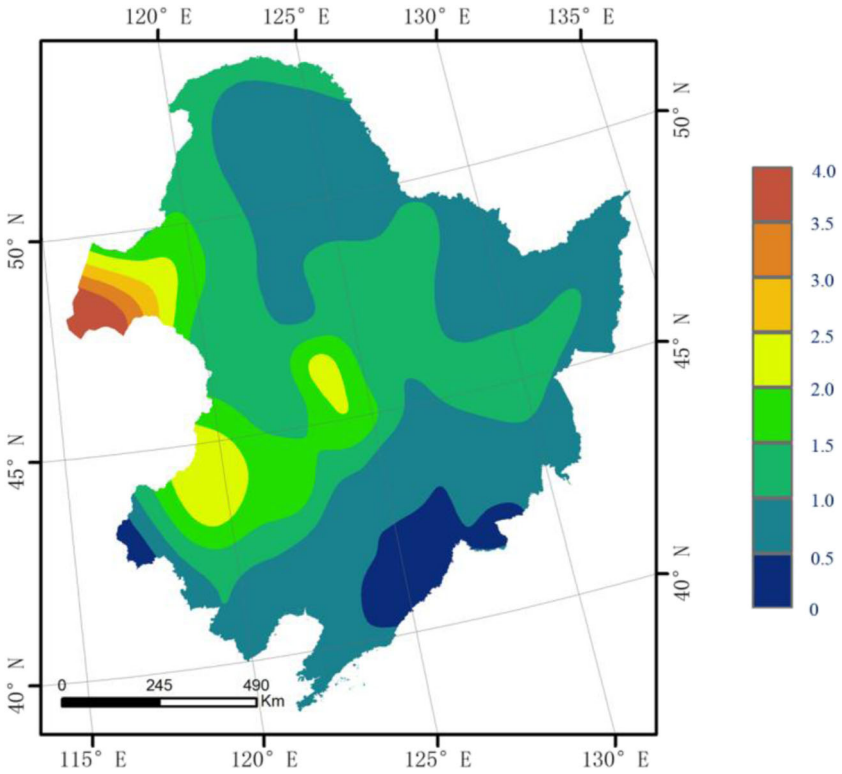


**Fig. 2** The climate aridity zones in Northeastern China

light, which is the function of $z$ (solar zenith angle), $b$ (wavelength), $od$ (the optical depth at 0.55 nm), and $amt$ (aerosol type) (Lucht et al. 2000). In this study, $S$ was derived from lookup table (LUT) generated by 6S model (http://geography.bu.edu/brdf/). The LUT, available from MODIS BRDF/albedo products homepage, contains $S$ values at different $z$, $b$, $od$, and $amt$ values. Parameters $z$ and $od$ were acquired from MOD03 and MOD04_L2, respectively, while $\alpha_w$ and $\alpha_b$ were acquired from MCD43B3. The aerosol types in the study area are continental type, as our study area is located in a

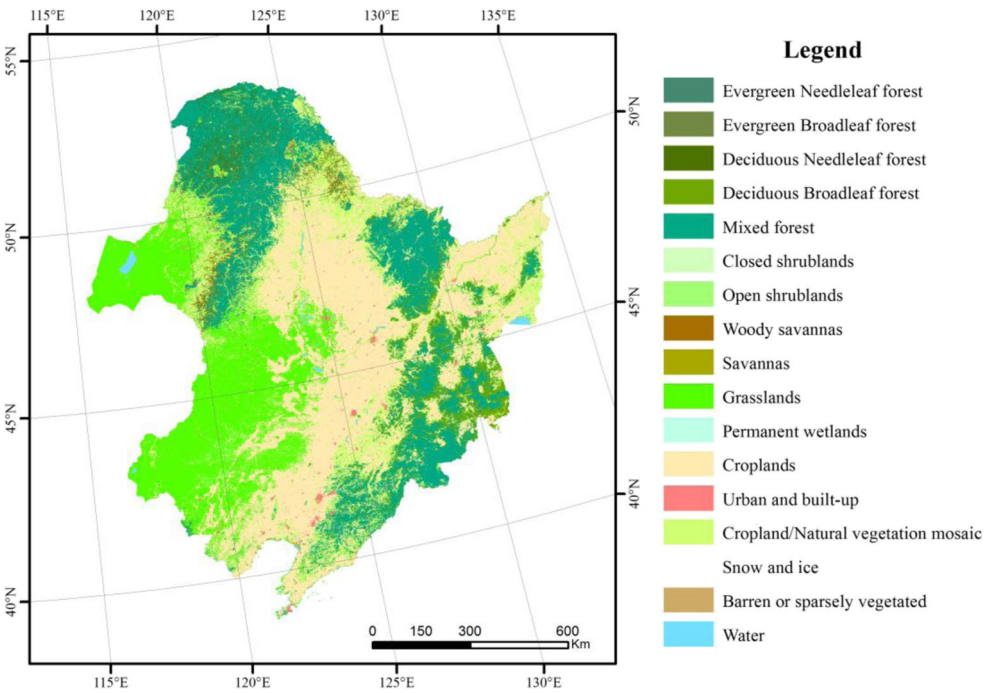


**Fig. 3** The land cover map of Northeastern China in 2010

continent; therefore, the *amt* was set up as 1 versus 0 as the oceanic type. In order to avoid the conversion of albedo from narrowband to broadband, this study calculated the real albedo directly using both white sky albedo and black sky albedo at shortwave band. Then the albedo data were acquired by the average monthly data and then replaced the value of each land cover types in the VEGPARM.TBL.

Leaf area index (LAI) is an important indicator for the canopy structure, representing the productivity of plant communities and directly affecting the interaction between land surface and atmosphere (McPherson 2007). We used the MOD15 product to acquire the spatial distribution of leaf area index and calculated the LAI of each land cover types in different seasons.

#### *2.2.3 Meteorological data and climate field data*

In this study, the meteorological station data and climate field data were required for driving the WRF model and testing the reliability of the simulated results, respectively. We obtained the daily average temperature data of July and December, 2010, from 101 stations covering the study area through China Meteorological Data Sharing Service System (CMDSS).We set the CMDSS data as the true temperature to assess the accuracy of our simulation. On the other hand, the climate field data, the every 6 h GRID 1 data, were downloaded from http://rda.ucar.edu from July 1 to 31 and from December1 to 31, which included 26 standard isobaric surface layers (1,000–10 hPa), the surface boundary layer (part of the R layer), and information from tropopause (e.g., pressure, temperature, relative humidity, etc.).

## 3 Method

The WRF model is a two-way nested mesoscale numerical weather prediction model which was designed to serve for idealized simulation, prediction, and regional climate research (Case et al. 2008). The model can be applied across scales from meters to thousands of kilometers, which is more appropriate to express the detailed regional characteristics than the regional climate model or global climate model.

In our study, four scenarios were designed to prove the impact of the deforestation on regional climate: In scenario 1, the land cover was in the original state and no farming land. Under this scenario, we replaced the agricultural land of the land cover data in 2010 with forest land and simulated the regional temperature from July 1 to July 31 of 2010. The land cover situation in scenario 2 was the current 2010 land cover while the simulation was set up from July 1 to July 31 of 2010. The land cover in scenarios 3 and 4 is the same as the scenarios 1 and 2, respectively, with the only difference in the simulation time from December 1 to 31 of 2010. The simulation result changed from scenarios 1 to 2 or from scenarios 3 to 4 showing the influence of the deforestation process on regional climate. All scenarios have three domains at the spatial resolutions 27, 9, and 3 km. The outermost domain (D01) at 27 km spatial resolution covered the entire region of Northeast Asia and western Pacific which would involve the impact of the summer monsoon and Mongolia high pressure system in winter. The domain is centered at 123.80° E, 47.55° N, including 152-by-152 grids. The middle domain (D02) at resolution 9 km covered 322-by-289 grids. The innermost domain (D03) covered our study area, Northeastern China, with the best resolution 3 km by 496-by-571 grids. The projection type of the three domains was lambert equal area azimuthal projection.

## 4 Results

### 4.1 The surface parameters at different seasons

#### *4.1.1 Albedo*

The surface albedo reflects the proportion of solar radiation absorbed by the surface, and it is one of the key factors which influence the regional and global climates (Barnes and Roy 2008; Li et al. 2013). Numerous studies and models have used a fixed value or a range to represent the albedo of each land cover type (Kvalevag et al. 2010). The WRF model provided two ways to acquire the spatial surface parameters: One is based on the derived remote sensing data, and the other is based on the vegetation parameter table. Although the remote sensing-derived data can provide more detailed information of the land surfaces, the surface parameters of the hypothetical scenarios cannot be derived from the satellite. The WRF model can use a maximum and minimum value to define the albedo of different land cover types, which provided a good way to obtain the spatial albedo maps of 4four scenarios. The initial data and parameters in WRF model were tried and tested mainly in America and Europe; more localized parameters are needed for our study area to make the simulation more accurate.

Based on the MCD43B3 data and other auxiliary data, we derived the authentic surface albedo of the study area in July and December 2010 (Fig. 4).

From the figure, we can see that the albedo in July changes from 0.01 to 0.24 with a clear spatial heterogeneity, correlating with land cover types. The albedo of cropland and grass land is higher than that of the forest land while the water body has the lowest value.

We used the spatial analysis tools of ArcGIS to calculate the average albedo on different land cover types at different seasons (July and December). The results are showed below in Table 1.

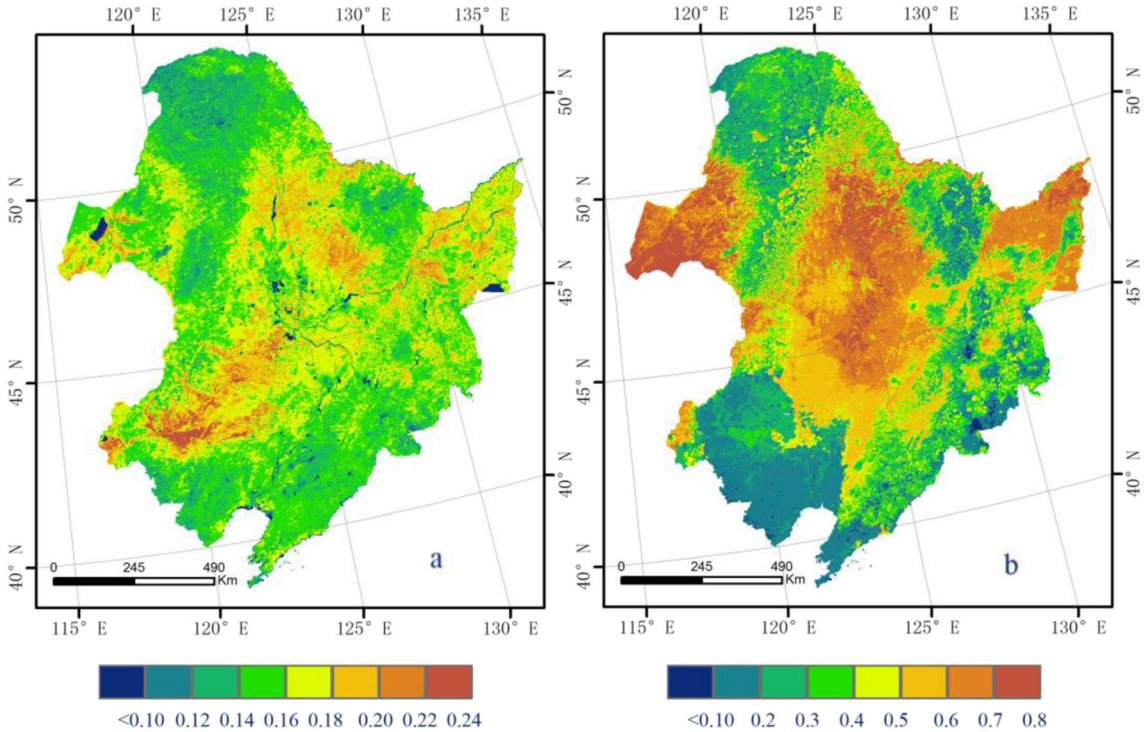


**Fig. 4** **a** The albedo maps of July; **b** the albedo maps of December

**Table 1** The albedo of different land covers at July and December

| Min albedo in July | Max albedo in July | Land cover types | Min albedo in Dec | Max albedo in Dec |
|---|---|---|---|---|
| 0.10 | 0.10 | Evergreen needleleaf forest | 0.21 | 0.22 |
| 0.12 | 0.12 | Evergreen broadleaf forest | 0.23 | 0.30 |
| 0.12 | 0.12 | Deciduous needleleaf forest | 0.30 | 0.32 |
| 0.15 | 0.16 | Deciduous broadleaf forest | 0.32 | 0.34 |
| 0.13 | 0.14 | Mixed forests | 0.27 | 0.28 |
| 0.13 | 0.14 | Closed shrublands | 0.50 | 0.52 |
| 0.13 | 0.13 | Open shrublands | 0.44 | 0.47 |
| 0.13 | 0.14 | Woody savannas | 0.36 | 0.37 |
| 0.13 | 0.14 | Savannas | 0.41 | 0.44 |
| 0.15 | 0.15 | Grasslands | 0.55 | 0.59 |
| 0.12 | 0.13 | Permanent wetlands | 0.53 | 0.58 |
| 0.16 | 0.17 | Croplands | 0.57 | 0.62 |
| 0.15 | 0.15 | Urban and built-up | 0.47 | 0.49 |
| 0.15 | 0.16 | Cropland/natural vegetation mosaic | 0.46 | 0.47 |
| 0.59 | 0.63 | Snow and ice | 0.59 | 0.63 |
| 0.38 | 0.38 | Barren or sparsely vegetated | 0.56 | 0.61 |
| 0.06 | 0.06 | Water | 0.58 | 0.60 |
| 0.15 | 0.20 | Wooded tundra | 0.15 | 0.20 |
| 0.15 | 0.20 | Mixed tundra | 0.15 | 0.20 |
| 0.25 | 0.25 | Barren tundra | 0.25 | 0.25 |

In Table 1, we can find that the surface albedo of December is significantly higher than that of July which can be attributed by the high albedo of the snow cover, especially on farming and grass lands whose albedo increased five to six times. The forest albedo have doubled, though not as obvious as the submerged vegetation land and the bare land because a seasonal snow covered the land surface which makes the surface turn into the physical properties of snow.

### *4.1.2 LAI*

Leaf area index (LAI) is a major indicator of plant growth conditions which can provide structured quantitative information of surface material and energy exchange for plant canopy and can largely influence the regional climate. Similar to the surface albedo, we get the heterogeneous spatial LAI maps (Fig. 5) of different seasons through remote sensing data.

In Fig. 5, we can easily find that the forest has higher LAI not only in July, but also in December, and a good correlation existed between LAI and land cover types. Therefore, we can use a fixed value or a range to represent the LAIs of land cover types (Table 2).

Table 2 showed the LAI of 20 land cover types in July and December. The rank of averaged LAI is forest, shrub lands, wetlands, croplands, grass land, barren land, and water in July. While in December the difference of LAI of land cover types is not clear and the LAI of land types are around 0, except the high LAI of the evergreen forest, even though it decreased dramatically.

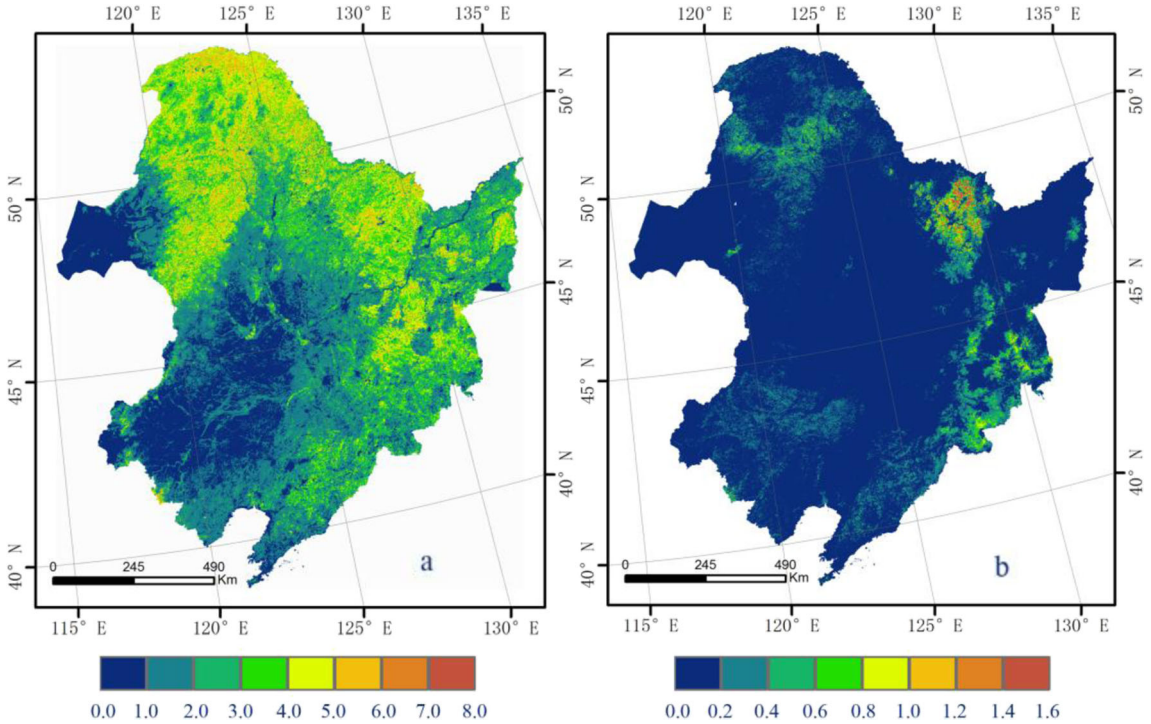


**Fig. 5** The spatial LAI maps derived from remote sensing in July (**a**) and December (**b**)

**Table 2** The maximum and minimum LAI of 20 land lover types in July and December

| LAIMIN in July | LAIMAX in July | Land cover types | LAIMIN in Dec | LAIMAX in Dec |
|---|---|---|---|---|
| 4.54 | 4.86 | Evergreen needleleaf forest | 0.09 | 0.20 |
| 2.53 | 4.20 | Evergreen broadleaf forest | 0.10 | 0.20 |
| 3.23 | 4.10 | Deciduous needleleaf forest | 0.10 | 0.22 |
| 2.41 | 4.46 | Deciduous broadleaf forest | 0.12 | 0.23 |
| 2.30 | 4.02 | Mixed forests | 0.04 | 0.18 |
| 2.67 | 3.21 | Closed shrublands | 0.10 | 0.10 |
| 1.00 | 1.18 | Open shrublands | 0.10 | 0.10 |
| 3.52 | 4.03 | Woody savannas | 0.10 | 0.12 |
| 3.06 | 3.83 | Savannas | 0.10 | 0.10 |
| 1.29 | 1.62 | Grasslands | 0.01 | 0.10 |
| 3.36 | 3.94 | Permanent wetlands | 0.10 | 0.10 |
| 1.60 | 2.51 | Croplands | 0.01 | 0.10 |
| 1.00 | 1.00 | Urban and built-up | 0.01 | 0.10 |
| 1.59 | 3.46 | Cropland/natural vegetation mosaic | 0.01 | 0.10 |
| 0.01 | 0.01 | Snow and ice | 0.01 | 0.01 |
| 0.10 | 0.75 | Barren or sparsely vegetated | 0.01 | 0.10 |
| 0.01 | 0.01 | Water | 0.01 | 0.01 |
| 0.41 | 3.35 | Wooded tundra | 0.01 | 0.10 |
| 0.41 | 3.35 | Mixed tundra | 0.01 | 0.10 |
| 0.41 | 3.35 | Barren tundra | 0.01 | 0.10 |

### 4.2 Authenticity test on the simulated temperature

We performed an accuracy test whether the model can simulate the real condition of the study area. We used the surface temperature collected from 101 meteorological stations to cover the study area to evaluate the simulation results from scenarios 1 and 3 in both July and December, respectively. The relationship between the simulated temperature and the observed temperature is shown in Fig. 6.

Figure 6a and b give us a clear description of the accuracy of simulations. Generally speaking, the simulated average temperatures of July are better than that of December which may be attributed to uncertainty and complexity of winter climate which caused the WRF dynamic framework cannot capture the temperature as well as the summer time. Specifically, the root mean square error and the mean bias of simulated average temperature in July are 0.2 and 0.3, and 1.2 and 1.3 in December. We found that most of high error points are located at regions with complex topography and high landscape heterogeneity. However, the best resolution in our simulation is 3 km which may have less detailed information, especially at heterogeneous region. The scale mismatch between 3 km resolution and point may also be the error source. Nonetheless, both the point pairs in July and December are closely around the function $y=x$ which represents a good consistency between simulated and observed data. Based on the agreement of temperatures, we assume that the WRF model and corresponding parameter schemes can obtain relatively accurate regional temperature and the temperatures

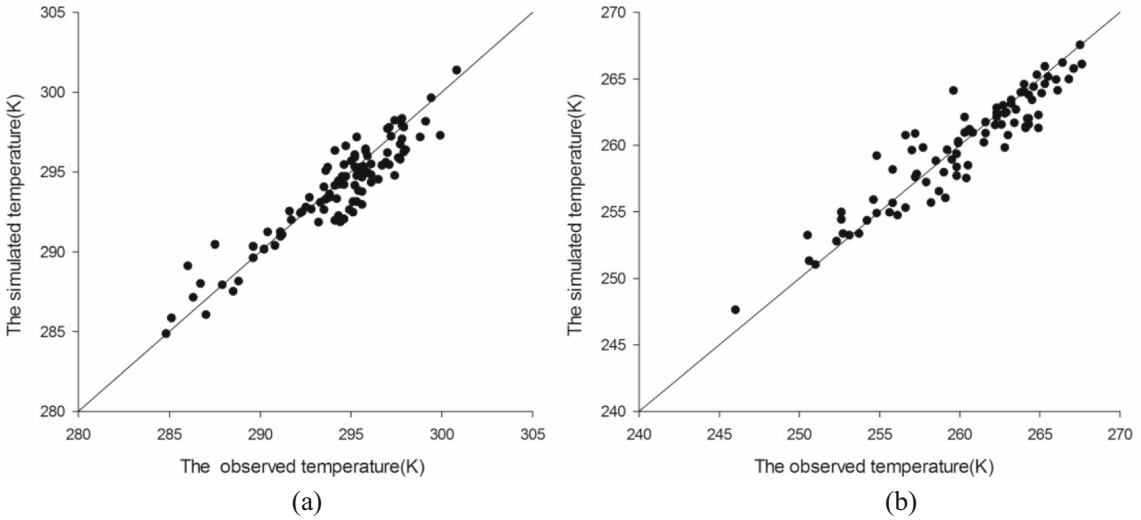


**Fig. 6** The difference between the simulated temperature and the temperature from stations. **a** The results in July; **b** the results in December

simulated in scenarios 1 and 3 are assumed to be the true value while the temperatures in scenarios 2 and 4 are the actual temperatures at the historical condition.

## 4.3 The impact of deforestation on temperature

### *4.3.1 The regional temperature effects caused by deforestation at different seasons*

According to "Section 3," we simulated the regional temperature under four scenarios with different land cover types with different physical parameters and different months. Simulation for all scenarios continued for a month, and average temperature during each analog was calculated to compare and show the spatial variability of regional temperature. The hypothesis in the method may help us understand that the climate change caused by deforestation can be displayed by the different temperatures between scenarios 1 and 2, and scenarios 3 and 4 in different months.

Figure 7 shows the result of temperature change between July and December. In Fig. 7, the temperature in the study area showed an overall downward trend along with the forest degradation. In July, the average regional temperature deceased 0.27 °C which should be considered as heterogeneity. The temperature at the point where land cover changes occurs decreased significantly, with the minimum temperature −1.78 °C. There is a slight temperature decrease in the surrounding land but not as obvious as the land cover changing land. In Fig. 7, we also found a slight temperature rise which might be caused by the interaction between canopies.

Compared with July, temperature decreased more than that of December, with the average temperature decreased 1.35 °C and the minimum value reaching −6.8 °C. From these two figures, we can find that the temperature in winter of the change area varied more remarkably than that in summer. This can be explained by the high albedo of snow cover, especially on farming or grass land and the deforestation process leading to sharp increase in albedo with less solar radiation and cooling climate. In summary, in both July and December, the deforestation process in our study area can decrease the regional temperature through the biological geophysical process.

It is also interesting to notice that the temperature changes on the deforestation land decreased from east to west, especially in July. For the study of the climate effects of land cover change, numerous studies have worked on the heat difference between latitudes which have different dominant physical process, albedo, or evapotranspiration, leading to different climate impacts. However, the vertical climate change due to the deforestation is worthy of careful consideration and verification. We will discuss it in the next section.

### *4.3.2 The temperature effects under different aridity conditions*

In the vertical profile, the aridity is a good indicator for climate change. Meanwhile, the humid or aridity condition determines the amount of plant transpiration which is critical in the physical process of how the land cover changes influences regional climate. Therefore, we calculated the temperature change at different aridity zones.

In order to detect the temperature change at different moisture conditions, we calculated the average temperature change where land cover has changed in three aridity zones. The average values are 0.2, 0.3 s and 0.4 °C at humid, semi-humid, and semi-aridity zones. Then we extracted the temperature changes of all the land cover changing points and displayed in Fig. 8.

In Fig. 8, we can see some coherences, as well as some differences between July and December. Generally, the

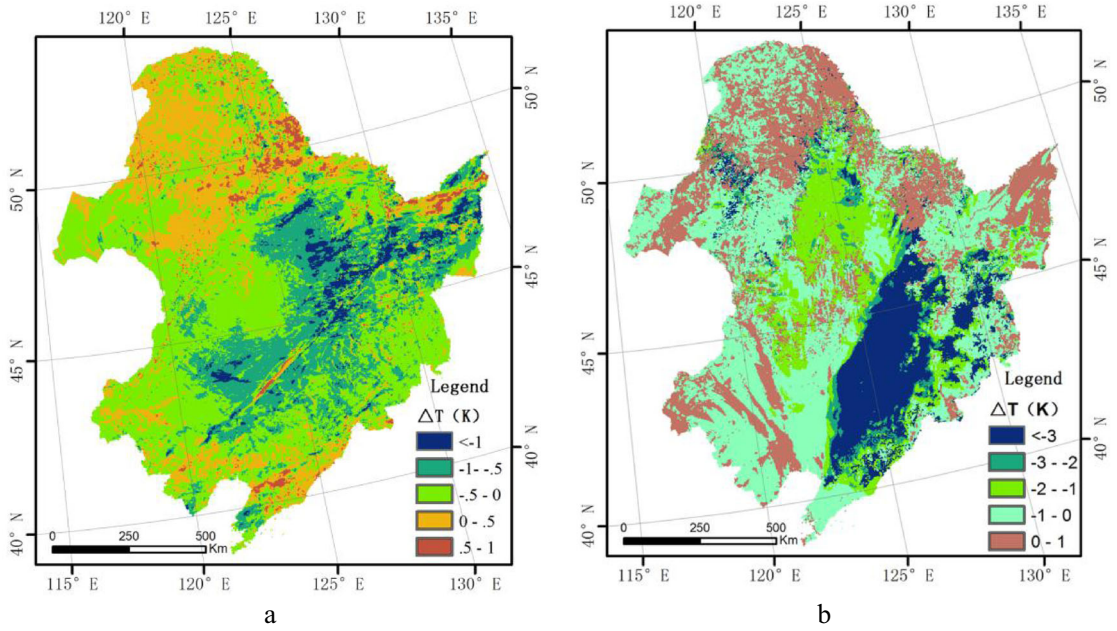


**Fig. 7** **a** The regional temperature change caused by deforestation in July; **b** the regional temperature change caused by deforestation in December

temperature decreased in all the aridity zones in both July and December because of the deforestation process. More than 80 % sample points in both summer and winter showed the cooling trend caused by the land cover change, demonstrating that the cooling outcome by increased albedo dominated more than the warming outcome caused by the increasing vegetation transpiration.

In July, the temperature in the semiarid area changed smaller than the semi-humid and humid areas. As the albedo was unrestricted to aridity, the change gradient of the temperature was attributed to the evaporation decrease of vegetation and soil. Therefore, the evapotranspiration of vegetation in the wetter areas with higher soil moisture is higher which implied higher latent heat flux and lower sensible heat flux through the Bowen ratio and thus cooling. In the Fig. 8a, we also can find a small amount (19.1 %) of points with increasing temperature in the deforested regions which can be explained by the complex interactions between the land surface and atmosphere and the edge effects.

In contrast to July, the average temperature changed in December are similar in the semi-arid areas while the average temperature decreased substantially, especially in the humid areas which can reach −4 °C or even more. Snow might be one reason for this. The wetter areas got more snow than the arid areas (seldom or not exists), which leads to higher albedo in humid areas, and reflects more solar radiation, resulting to the higher intense temperature decrease. Therefore, in the perspective of the protection and rational allocation of land, more attention should be paid to the wetter areas as the land cover changes may cause more serious climate responses.

## 5 Conclusion and discussion

According to the Betts et al. (2007) study, it may be less useful to represent the local short radiative forcing caused by anthropogenic surface albedo change and the local surface moisture budget changes caused by surface roughness, leaf area index,

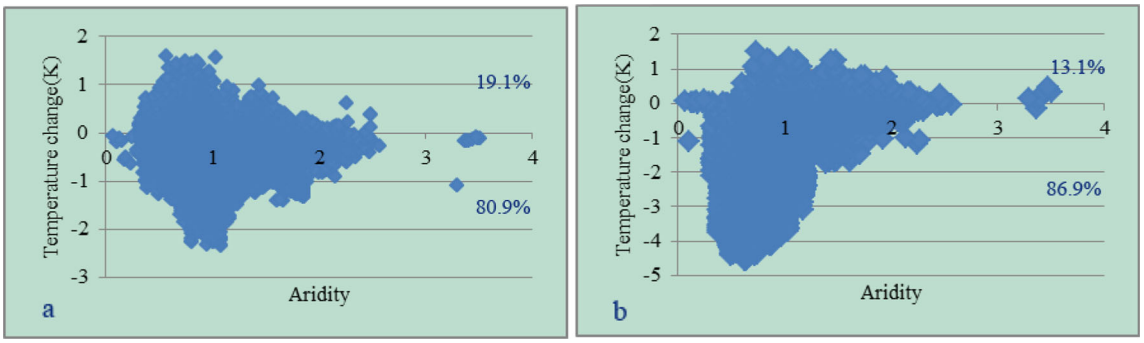


**Fig. 8** **a** The temperature changes at different aridity intervals in July; **b** the temperature changes at different aridity intervals in December

and rooting depth through global mean results simulated by global climate models such as GCMs. Therefore, the information on regional climate changes is required in order to better understand the mechanism and consequences of climate changes caused by typical land cover changes on regional scale.

In this study, we designed four scenarios for WRF to compare and analyze the climate influences caused by deforestation in different seasons and aridity conditions on regional scale. We took advantage of previous studies' land cover data in Northeastern China and the MODIS products such as MCD43B3 and MOD15 with high spatial and temporal resolution to replace the land surface parameters in the initialization of WRF to make the simulation more localized.

The temperature in both summer and winter showed a decreasing trend when the conversion of forest to farmland occurred in Northeastern China. This indicated that the albedo change caused by land cover changes appears to be the dominant biogeophysical effect on regional temperature, especially in snow-masked seasons, which is inconsistent with the conclusion that the shortwave radiative forcing due to surface albedo change can exceed $-5\ Wm^{-2}$ in mid-latitude areas such as North America and cooler regions of Asia, as from Betts et al. (2007) and Lamptey et al. (2005). The land cover conversion from forest to cropland can decrease the leaf area index and rooting depth which allowed less evapotranspiration and implied reduced latent heat flux, leading to warming climate. The temperature change in summer being relatively small is the offset between the two effects and showed even in summer days that the albedo change plays a greater role. This conclusion also illustrated that the land cover conversion influences on regional temperature in the Northeastern China may have more agreement with the boreal area than the tropical areas.

Finally, the temperature change in different aridity conditions including semi-arid, semi-humid, and humid zones were analyzed. Under the humid zones, the temperature decreased more than the other two zones, especially in December when the decreased temperature reached 4–5 °C. This can be explained by two aspects: On the one hand, the wetter areas got more snow than the arid areas (seldom or not exists) which leads to higher albedo in humid areas and reflects more solar radiation, resulting in the high, intense temperature decrease; on the other hand, the evapotranspiration of vegetation in the wetter areas with higher soil moisture is higher, which implied higher latent heat flux and lower sensible heat flux through the Bowen ratio and thus cooling. This question of why the difference of temperature change between aridity zones exists is still not certain, and should be further studied in our following works. However, in perspective of the protection and rational allocation of land, more attention should be paid to the wetter areas in which the land cover changes can contribute to more serious climate responses.

## References


Baidya Roy S (2003) Impact of historical land cover change on the July climate of the United States. J Geophys Res 108(D24)

Bala G et al (2007) Combined climate and carbon-cycle effects of large-scale deforestation. Proc Natl Acad Sci U S A 104(16):6550–6555

Barnes CA, Roy DP (2008) Radiative forcing over the conterminous United States due to contemporary land cover land use albedo change. Geophys Res Lett 35(9)

Barnes CA, Roy DP (2010) Radiative forcing over the conterminous United States due to contemporary land cover land use change and sensitivity to snow and interannual albedo variability. J Geophys Res-Biogeosci 115(G04033)

Betts RA (2001) Biogeophysical impacts of land use on present-day climate: near-surface temperature change and radiative forcing. Atmos Sci Lett 2(1–4):39–51

Betts RA et al (2007) Biogeophysical effects of land use on climate: Model simulations of radiative forcing and large-scale temperature change. Agric For Meteorol 142(2–4):216–233

Bonan GB (1997) Effects of land use on the climate of the United States. Clim Chang 37(3):449–486

Bonan GB (2008) Forests and climate change: Forcings, feedbacks, and the climate benefits of forests. Science 320(5882):1444–1449

Bounoua L et al (2002) Effects of land cover conversion on surface climate. Clim Chang 52(1–2):29–64

Case JL et al (2008) Impacts of high-resolution land surface initialization on regional sensible weather forecasts from the WRF model. J Hydrometeorol 9(6):1249–1266

Collins WD et al (2006) The Community Climate System model version 3 (CCSM3). J Clim 19(11):2122–2143

Comarazamy DE et al (2013) Climate impacts of land-cover and land-use changes in tropical islands under conditions of global slimate shange. J Clim 26(5):1535–1550

Cooley HS et al (2005) Impact of agricultural practice on regional climate in a coupled land surface mesoscale model. J Geophys Res-Atmos 110(D3)

Correia FWS et al (2007) Modeling the impacts of land cover change in Amazonia: a regional climate model (RCM) simulation study. Theor Appl Climatol 93(3–4):225–244

Dai L et al (2006) The roles of a decision support system in applying forest ecosystem management in Northeast China. Sci China Ser E 49(Supp.I):9–18

Das SK et al (2011) Climate change studies using coupled model: land surface perspective. J Indian Soc Remote Sens 39(3):323–336

Davin EL, de Noblet-Ducoudré N (2010) Climatic impact of global-scale deforestation: radiative versus nonradiative processes. J Clim 23(1): 97–112

Deng XZ et al (2013)"Systematic modeling of impacts of land use and land cover changes on regional climate: a review." Adv Meteorol

Dirmeyer PA et al (2010) Impacts of land use change on climate. Int J Climatol 30(13):1905–1907

Feddema J et al (2005a) A comparison of a GCM response to historical anthropogenic land cover change and model sensitivity to uncertainty in present-day land cover representations. Clim Dyn 25(6): 581–609

Feddema JJ et al (2005b) The importance of land-cover change in simulating future climates. Science 310(5754):1674–1678

Fu C (2003) Potential impacts of human-induced land cover change on East Asia monsoon. Glob Planet Chang 37(3/4):219–229

Hahmann AN, Dickinson RE (1997) RCCM2-BATS model over tropical South America: applications to tropical deforestation. J Clim 10(8): 1944–1964

Kvalevag MM et al (2010) Anthropogenic land cover changes in a GCM with surface albedo changes based on MODIS data. Int J Climatol 30(13):2105–2117

Lamptey BL et al (2005) Impacts of agriculture and urbanization on the climate of the Northeastern United States. Glob Planet Chang 49(3–4):203–221

Lawrence DM et al (2007) The partitioning of evapotranspiration into transpiration, soil evaporation, and canopy evaporation in a GCM: Impacts on land-atmosphere interaction. J Hydrometeorol 8(4): 862–880

Li Z, Molders N (2008) Interaction of impacts of doubling CO(2) and changing regional land-cover on evaporation, precipitation, and runoff at global and regional scales. Int J Climatol 28(12):1653–1679

Li H et al (2013) Field measurement of albedo for different land cover materials and effects on thermal performance. Build Environ 59: 536–546

Lucht W et al (2000) An algorithm for the retrieval of albedo from space using semiempirical BRDF models. IEEE Trans Geosci Remote Sens 38(2):977–998

Mahmood R et al (2006) Land use/land cover change and its impacts on climate. Glob Planet Chang 54(1-2):vii–vii

Mahmood R et al (2010) Impacts of land use/land cover change on climate and future research priorities. Bull Am Meteorol Soc 91(1):37–46

McPherson RA (2007) A review of vegetation–atmosphere interactions and their influences on mesoscale phenomena. Prog Phys Geogr 31(3):261–285

Niyogi D et al (2009) Land-use/land-cover change and its impacts on weather and climate. Bound-Layer Meteorol 133(3):297–298

Paeth H et al (2009) Regional climate change in tropical and Northern Africa due to greenhouse forcing and land use changes. J Clim 22(1):114–132

Sitch S et al (2005) Impacts of future land cover changes on atmospheric CO2 and climate. Glob Biogeochem Cycles 19(2)

Steiner AL et al (2005) The coupling of the Common Land Model (CLM0) to a regional climate model (RegCM). Theor Appl Climatol 82(3–4):225–243

Subin ZM et al (2011) "Ecosystem feedbacks to climate change in California: development, testing, and analysis using a coupled regional atmosphere and land surface model (WRF3-CLM3.5)." Earth Interactions 15: doi: doi:10.1175/2010EI331.1

Swann AL et al (2010) Changes in Arctic vegetation amplify high-latitude warming through the greenhouse effect. Proc Natl Acad Sci U S A 107(4):1295–1300

Wang S et al (2010) Land use and landscape pattern changes in Nenjiang River Basin during 1988–2002. Front Earth Sci-Prc 4(1):33–41

Wang Y et al (2013) Simulation of the influence of historical land cover changes on the global climate. Ann Geophys 31(6):995–1004

Wu F et al (2013) "Land cover mapping based on multisource spatial data mining approach for climate simulation: a case study in the farming–pastoral ecotone of North China." Adv Meteorol

Ye B et al (2001) The driving forces of land use/cover change in the upstream area of the Nenjiang River. Chines Geogr Sci 11(4): 377–381

Zeng XM, Wu ZH, Xiong SY et al (2011) Sensitivity of simulated short-range high-temperature weather to land surface schemes by WRF. China Earth 54:581–590

Zhang H et al (2008) Climate impacts of land-use change in China and its uncertainty in a global model simulation. Clim Dyn 32(4):473–494